Usoi Dam Wave Overtopping and Flood Routing in the Bartang and Panj Rivers, Tajikistan

**Prepared in cooperation with the
U.S. Agency for International Development,
Office of U.S. Foreign Disaster Assistance**

Water-Resources Investigations Report 03-4004

Cover photograph:

The Usoi dam was created in the winter of 1911 after an earthquake caused a rock slide that completely blocked the valley of the Bartang River in the Pamir Mountains of southeastern Tajikistan. At present the dam impounds 17 million cubic meters of water in Lake Sarez. A major flood emanating from Lake Sarez could be devastating to millions of people downstream, not only in Tajikistan but also in Afghanistan, Uzbekistan, and Turkmenistan. (Photograph courtesy of the National Aeronautics and Space Administration, Johnson Space Center, Image Science and Analysis Laboratory.)

Usoi Dam Wave Overtopping and Flood Routing in the Bartang and Panj Rivers, Tajikistan

By John Risley, Joseph Walder, and Roger Denlinger

Water-Resources Investigations Report 03-4004

U.S. Department of the Interior
U.S. Geological Survey

Contents

Figures

Tables

Conversion Factors

Multiply	By	To obtain
millimeter (mm)	0.03937	inch
meter	3.281	foot
kilometer (km)	0.6214	mile
square kilometer (km2)	0.3861	square mile
cubic meter (m^3)	1.308	cubic yard (yd^3)
cubic meter per second(m^3/s)	35.31	cubic foot per second (ft^3/s)

Temperature in degrees Fahrenheit (°F) is calculated as follows:

$$°F = (1.8°C+32)$$

In this report vertical coordinates are referenced to the National Geodetic Vertical Datum of 1929 (NGVD of 1929)—a geodetic datum derived from a general adjustment of the first-order level nets of both the United States and Canada.

This page is intentionally blank.

Usoi Dam Wave Overtopping and Flood Routing in the Bartang and Panj Rivers, Tajikistan

By John Risley, Joseph Walder, and Roger Denlinger

Abstract

The Usoi dam was created in the winter of 1911 after an enormous seismogenic rock slide completely blocked the valley of the Bartang River in the Pamir Mountains of southeastern Tajikistan. At present the dam impounds 17 million cubic meters of water in Lake Sarez.

Flood volume and discharge estimates were made for several landslide generated floods that could overtop the dam. For landslide volumes of 200, 500, and 1,000 million cubic meters, estimated overtopping flood volumes were 2, 22, and 87 million cubic meters of water, respectively. Estimated peak discharge at the dam for these three flood scenarios were 57,000, 490, 000, and 1,580,000 cubic meters per second, based on triangular hydrographs of 70-, 90-, and 110-second durations, respectively.

Flood-routing simulations were made for the three landslide-induced overtopping floods over a 530-kilometer reach of the Bartang and Panj Rivers below the Usoi dam. A one-dimensional flow model using a Riemann numerical solution technique was selected for the study. A constant 50-meter wide rectangular channel, which represented the mean channel width, was used for the entire reach. A roughness coefficient of 0.038, appropriate for steep mountainous streams, also was used for the entire reach.

For the 87 million cubic meter volume overtopping flood scenario, the peak flows were approximately 1,100, 800, and 550 cubic meters per second at locations 50, 100, and 150 kilometers downstream of the dam, respectively.

The model was also used to simulate the less likely scenario of an instantaneous dam breach and draining of the total volume of the lake. Simulated peak flows were approximately 64,000, 52,000, 40,000, and 20,000 cubic meters per second at locations 50, 100, 150, and 530 kilometers downstream of the Usoi dam.

Introduction

In the winter of 1911 an enormous seismogenic rock slide completely blocked the valley of the Bartang River in the Pamir Mountains of southeastern Tajikistan (fig. 1) (Alford and Schuster, 2000). The Usoi landslide dam, named after a village that was buried by the slide, is the highest dam—natural or man made—in the world. Following emplacement of the Usoi landslide dam, which has a thickness of 500 to 700 m, a lake (Lake Sarez) began to form behind the dam. For the first few years after

impoundment, water level rose at a rate of approximately 75 meters per year. Today Lake Sarez is more than 60 kilometers long, has a maximum depth in excess of 500 meters, and contains an estimated 17 cubic kilometers of water. The lake-surface elevation is higher than 3,000 meters above sea level. Surrounding mountains peaks reach elevations higher than 6,000 meters. The current freeboard (distance between the lake surface and the lowest point on the dam crest) is approximately 50 meters. Lake level is currently rising at an average of 0.2 meters per year, and approximately 50 to 60 cubic meters per second of water leak through the dam.

Figure 1. Study area reach

     Many landslide dams have failed, producing catastrophic floods (Costa and Schuster, 1991), so, unsurprisingly, the potential for catastrophic drainage of Lake Sarez has been a concern for many decades. Since the political disintegration of the Soviet Union, Western scientists and disaster-management experts have become involved in evaluating hazards associated with Lake Sarez. Depending on the magnitude of the event, a flood emanating from Lake Sarez could be devastating to people downstream, not only in Tajikistan but also in Afghanistan, Uzbekistan, and Turkmenistan. To mitigate potential disaster, Tajik officials and Western disaster-management experts want to develop an early warning system for the Bartang and Panj River Valley region and improve the infrastructure required for better disaster preparedness. U.S. Geological Survey (USGS) is assisting in the development of the early warning system.

Results from previous geotechnical studies (Hanisch and Soder, 2000; Stucky Consulting Engineers, 2001) indicate that the Usoi dam itself is unlikely to fail owing to either seismic shaking or ground-water seepage forces. The likeliest scenario for a flood involves landslide-generated water waves overtopping the dam. A rock mass on the right-bank slope of the lake, approximately 3 kilometers from the dam, is known to be creeping slowly and is one obvious potential source of a wave-generating landslide (fig. 2; Alford and Schuster, 2000). As we will show below, the volume of water in an overtopping flood wave would depend on landslide characteristics (including volume), geometry of the dam, freeboard, and the proximity of the landslide to the dam. Waves overtopping the dam would generate floods downstream and, if sufficiently erosive, might breach the dam, resulting in a secondary flood involving a substantial portion or all of the water impounded.

Figure 2. Lake Sarez and the Usoi Dam

Purpose and Scope

We used physically based models to estimate the flood hydrograph *at the dam* for a range of overtopping flood events as well as for catastrophic dam failure. These results were upstream boundary input for flood-routing simulations between the Usoi dam and the town of Moskovskiy (approximately 530 kilometers downstream) to determine peak flow depths and flood-wave travel times. The flood-routing simulations were made using a one-dimensional computational model developed by Denlinger and Iverson (2001), which uses a Riemann technique (Toro, 1997). Results of this study will assist in the development of an early warning system, which is one component of overall USGS activities related to hazards at Lake Sarez. Other USGS activities include providing computer hardware, software, and training in the Geographic Information System (GIS) applications to Tajik officials and disaster-management specialists.

Investigations related to the work reported here have been carried out by Alford (2000) and Stucky Consulting Engineers (2001). Alford (2000) assumed certain flood volumes and applied the U.S. National Weather Service FLDWAV hydraulic model (formerly known as DAMBRK) to route the hypothetical floods a distance of 184 kilometers (km) downstream. Stucky Consulting Engineers (2001) applied methods different from ours to estimate the probable volume of water that would

overtop the Usoi dam owing to landslides into Lake Sarez. They concluded that landslide-generated overtopping floods would be considerably more modest than the scenarios that we suggest. A comparison of the differing overtopping flood magnitudes is presented in Appendix A.

Description of the Study Area

The geology of the Pamir Mountains in the vicinity of Lake Sarez is described briefly by Fan and Wallace (1994). Geotechnical assessments (Hanisch and Soder, 2000) have identified at least one potentially unstable rock mass along the lake shore, but broader-scale geotechnical assessments have not been done.

For flood-routing purposes, we considered the reach extending approximately 530 kilometers along the Bartang and Panj Rivers from Lake Sarez to Moskovskiy (fig. 1). The Panj River in this reach forms the international border between Tajikistan and Afghanistan. This region of Tajikistan is extremely mountainous and arid. Mean annual precipitation at the Lake Sarez hydrometeorological station (elevation 3,290 meters) is 108 millimeters, and mean annual ambient air temperature at the station is 1 degree Celsius (Watanabe, 2000). The lake elevation is approximately 3,265 meters above mean sea level, while the elevation of the river at Moskovskiy is 582 meters above mean sea level. Overall, the study reach has an mean channel gradient of 0.47 percent. The upper section of the study reach (Bartang River) is from the Usoi dam to the Panj River confluence. This section is approximately 150 kilometers in length and has a mean channel gradient of 0.74 percent. Geomorphic features along the Bartang River include glacial moraines, river terraces, alluvial fans/cones, flood plains, talus slopes, and steep bedrock valley margins. The lower section of the study reach (Panj River) is approximately 380 kilometers in length and has a mean gradient of 0.37 percent. A longitudinal bed-channel profile of the entire study reach, based on data from a Digital Elevation Model (DEM) of the study area that was created in an earlier phase of the study, is shown in figure 3.
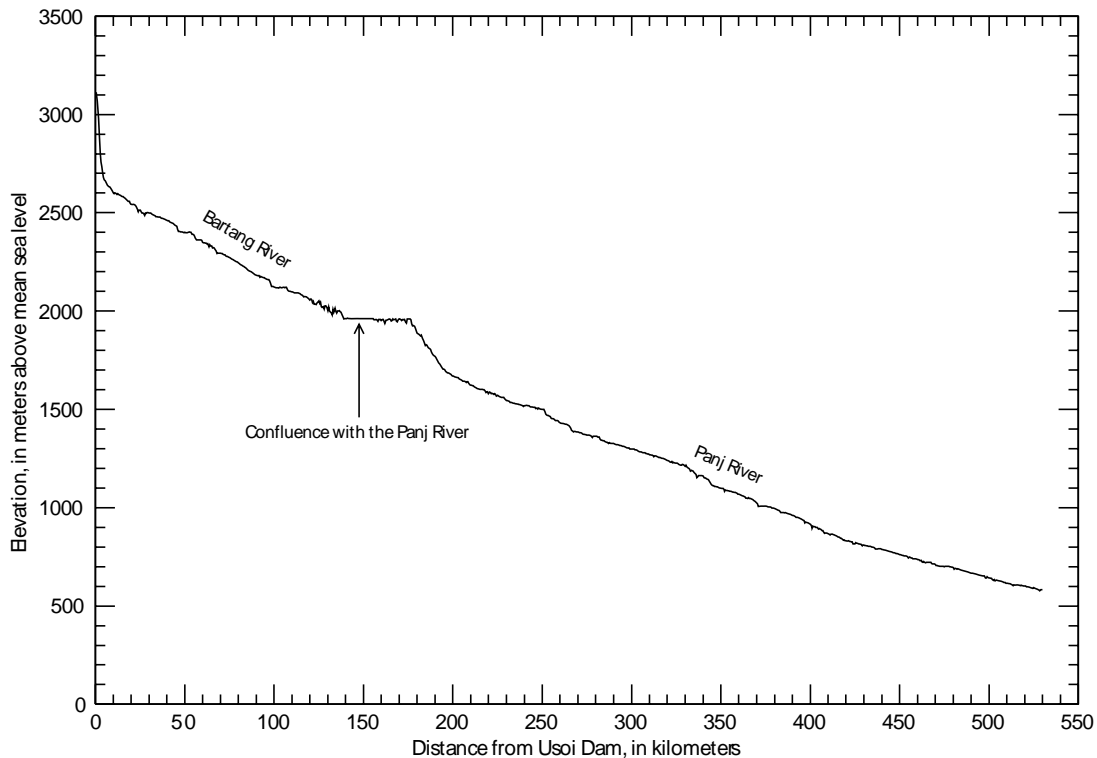
Figure 3.--Bartang-Panj River reach longitudinal bed-channel profile.
[Source: U.S. Geological Survey, Digital Elevation Model developed for the study.]

The economy of the study area is predominately agrarian. The main crops are potatoes and cereals. Owing to the rugged terrain, many farms and dwellings lie on the only arable land available: alluvial fans and terraces close to the river. An estimated 35,000 or more inhabitants of the Bartang and Panj River valleys could be affected by even a moderate flood outburst (Ives and Pulatova, 2000).

Acknowledgments

The authors thank Janice Fulford of the USGS Hydrologic Instrumentation Facility for her assistance in this project.

Probable Flood Hydrograph Determination

The likely sources of floods emanating from Lake Sarez include overtopping waves generated by landslides into the lake or a less likely total dam breach. We evaluate plausible scenarios for each of these mechanisms. The resulting hypothetical floods at the dam are then taken as starting conditions for downstream flood-routing describe in a subsequent section.

Landslide-Generated Floods

To address the possibility of landslide-generated waves overtopping the dam, we used results of Walder and others (in press) to relate landslide characteristics to wave amplitude, along with Synolakis' (1987) method for computing wave runup and Müller's (1995) results relating overtopping flood volume to runup and freeboard. The following is a summary of the method, which requires us to evaluate three phenomena: wave generation, wave runup, and wave overtopping. A more detailed presentation of the method, including pertinent mathematics, is presented in Appendix B.

Wave Generation

The experimentally based scaling results of Walder and others (in press) form a starting point for predicting the "near-field" wave amplitude associated with a particular size landslide. ("Near field" refers to the region just beyond the "splash zone" of complicated fluid/solid interaction, but before propagation effects become dominant.) Wave amplitudes predicted by this method strictly apply to only two-dimensional (flume-like, using the x and z dimensions) geometry. The situation at Lake Sarez obviously differs from a flume, as the likely landslide sources are along the banks. This fact has two consequences: First, the impulse wave set up by a landslide would spread laterally during the time of landslide motion. Second, the near-field wave mound will then "split" and propagate both towards the Usoi dam and towards the opposite end of the lake. We deal with the second of these factors simply by doubling the landslide volume associated with a given wave height via a flume analysis. To deal with lateral wave spreading during submerged landslide motion, it was assumed that the near-field wave source evolves into more or less a circular mound and conserves the total wave volume, as described in the TOPICS software package (Watts, 2001). For purposes of characterizing the wave source, we assume that water depth in the wave generation region is about 350 m.

Wave Runup

We assume as a reasonable approximation that Synolakis' (1987, 1991) results for runup of solitary waves are applicable to the impulse waves of interest here. Solitary waves constitute a special class of impulsively generated waves (e.g., Dean and Dalrymple, 1991), and while the impulse waves studied experimentally by Walder and others (in press) and previous investigators were not strictly solitary waves, we are unlikely to be making a great error by applying Synolakis' results. Runup is defined as the highest point (relative to the ambient water surface) that would be reached by a wave as it runs into an indefinitely long sloping plane. If runup R exceeds freeboard f, the elevation difference between ambient water level and the dam crest, then water must spill over the dam crest. The upvalley face of the Usoi dam obviously is not planar, but for purposes of applying Synolakis' results, we assume a uniform embankment slope of 23 degrees, a value estimated by inspection of a topographic map of the dam.

Overtopping

The results of Müller (1995) may be used to estimate the overtopping flood characteristics. Müller did flume experiments with solitary waves generated by a falling mass and dams with diverse embankment slopes and crest widths. He found that the last two factors had relatively little effect on overtopping flood volume, which depended primarily on freeboard, runup, and wave height. Because wave height depends on landslide volume and runup height depends upon wave height, one can derive

an expression relating overtopping flood volume to landslide volume and freeboard. Müller's results were also applied to estimate the duration of overtopping. Details are presented in Appendix B.

The Usoi landslide dam is of course not a simple embankment, and the freeboard varies from point to point. To apply Müller's results, we estimated an "average" freeboard as follows: For any specified runup height, the wave would overtop the dam crest between, say, s*1* and s*2*, where *s* is a coordinate measured along the mean strike of the dam crest. The average freeboard f*average* was then defined simply as the mean value of *f* in the interval between s*1* and s*2*. The total overtopping flood volume was then computed as the overtop flood volume per unit width for freeboard f*average* times the width of the dam crest actually overtopped.

The tabulated peak discharge is estimated by assuming a simple triangular hydrograph with identical rising and falling limbs. Table 1 and ure 4 show the characteristics of three overtopping flood hydrographs resulting from volumes of 200, 500, and 1,000 million cubic meters of landslide debris falling into the lake. The volume of water that overtops the dam is only about 0.5 percent of the total lake volume for the largest landslide considered.

Table 1: Summary of overtopping flood characteristic

Landslide volume, in million cubic meters	Overtopping flood volume, in million cubic meters	Overtopping flood duration, in seconds	Peak discharge at dam, in cubic meters per second
200	2	70	57,000
500	22	90	490,000
1000	87	110	1,580,000
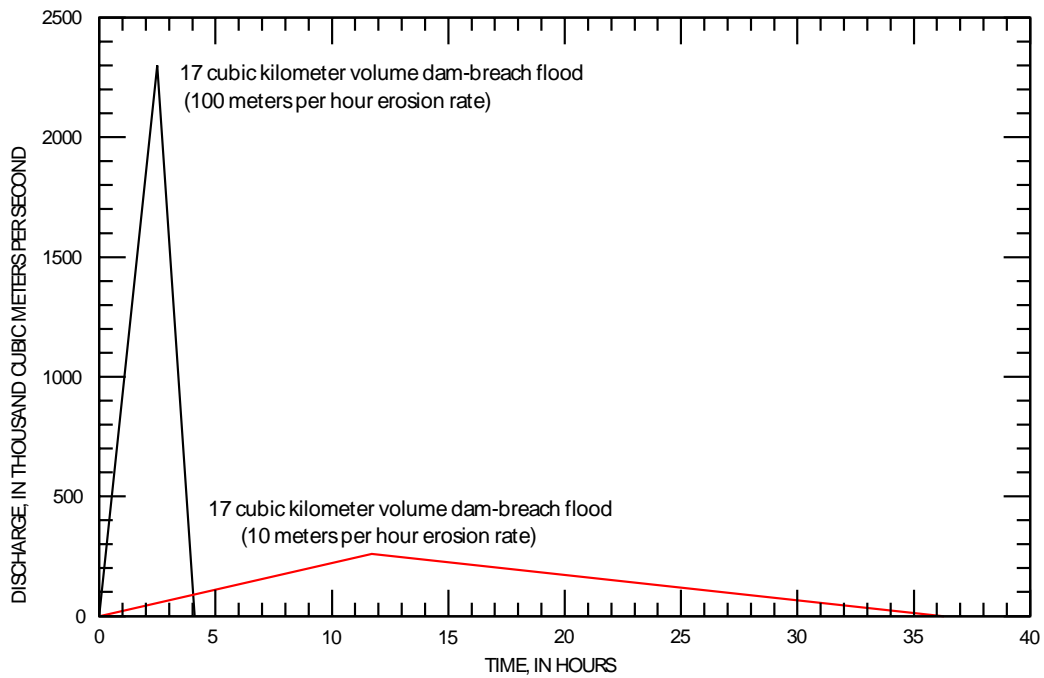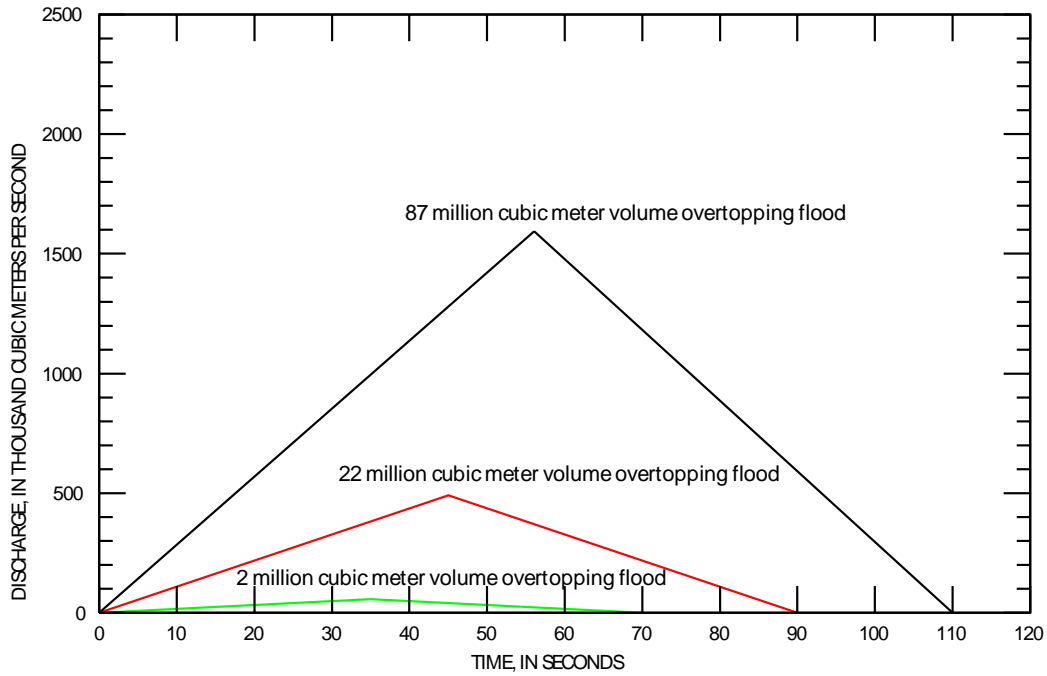
Figure 4.--Hydrographs showing change in discharge with time for overtopping and dam-breach floods.

Dam Breach Flood

The possibility of catastrophic dam breaching and drainage of the entire lake is unlikely (Hanisch and Soder, 2000; Stucky Consulting Engineers, 2001), but because the resulting flood would be much larger than one resulting from a wave overtopping the dam, a hypothetical breach flood bears investigation. Geotechnical studies suggest that the Usoi dam is unlikely to fail owing to either seismic shaking or ground-water seepage forces (Hanisch and Soder, 2000; Stucky Consulting Engineers, 2001). However, sufficiently large landslide-generated water waves would overtop the dam and perhaps erode the blockage enough to initiate a breach. This type of breach has been documented to have occurred in Italy (Costa, 1991), Canada (Clague and Evans, 1994), and Oregon, United States (O'Connor and others, 2001). Plausible bounds on the starting hydrograph for a breach flood may be readily derived from Walder and O'Connor (1997), who showed that peak flow may be related to total lake volume, a characteristic lake depth, and an average erosion rate of the breach. In table 2 below and in figure 4, the lower bound on peak discharge corresponds to an assumed breach erosion rate of 10 meters per hour (m/h), while the upper bound corresponds to as assumed breach erosion rate of 100 m/h. Walder and O'Connor (1997) found from their literature review that estimated erosion rates for actual dam failures nearly all fell within this range. More details on this method are presented in Appendix C.

Table 2: Summary of dam-breach flood characteristics

Erosion rate, in meters per hour	Peak discharge at dam, in million cubic meters per second	Time to peak flow, in hours	Time to empty lake, in hours
10	0.26	11.7	36.3
100	2.3	2.5	4.1

Flood Routing

The flood-routing component of the study included selecting a flood-routing model and defining proper channel hydraulic characteristics, and performing simulations for the possible flood hydrographs at the dam.

Model Selection

Four separate one-dimensional dynamic hydraulic models were evaluated for suitability in simulating the overtopping flood scenarios listed in table 1. These models included U.S. National Weather Service FLDWAV (formerly known as DamBreak) (Fread and Lewis, 1998), USGS-FourPt (DeLong and others, 1997), USGS-DAFLOW (Jobson, 1989), and a USGS one-dimensional flow model developed by Denlinger and Iverson (2001). Each of these models were tested using the worst-case overtopping flood scenario, in which a massive landslide (1 cubic kilometer in volume) generates a 110-second triangular flood hydrograph with a peak discharge of 1,580,000 cubic meters per second (a total volume of 87 million cubic meters of water) at the upstream boundary. A hypothetical model configuration having a length of 530 kilometers, constant width, and 0.47 percent gradient was used in each test. Of the models tested, only the model developed by Denlinger and Iverson (2001) succeeded

in fully simulating the downstream propagation of the flood wave from start to finish. The other models could not process flow input data from the 110-second triangular hydrograph, and subsequently terminated their simulations after only a few time steps. Accordingly, the model developed by Denlinger and Iverson (2001), which will be referred to as the "Denlinger model" in this report, was used for flood-routing simulations in the study.

Model Description

The Denlinger model numerically solves the one-dimensional shallow-water equations (or St. Venant equations) as described in Vreugdenhil (1994). The equations were solved using an approximate weighted average flux Riemann solver (Toro, 1997) with a fractional step correction for the source term created by bottom topography and for the influence of bed friction. Bed friction was parameterized by a Manning roughness coefficient (described in a following section). The initial conditions are a rectangular prism of water at rest upstream of a dry channel. Once the water is released, it rapidly forms an approximate triangular wave, and the user selects the length, width, and height of the prism to produce a wave with the specified total volume of discharge at the dam. The flow is then routed downstream along the channel thalweg. The time step length is based on the Courant number and can vary during a simulation. (The Courant number is the cell size divided by the sum of the fluid speed and the gravity wave speed.) Time steps typically range from 0.01 to 20 seconds in length.

Channel Configuration

Cross sections were delineated from a 17-meter-cell sized DEM of the study area and equally spaced every 0.5 kilometers along the channel thalweg. The DEM encompassed the entire 530 kilometer study reach with 10-kilometer buffer width. The DEM was created by scanning and vectorizing 1:50,000 scale Soviet General Staff topographic maps with 20-meter contour intervals. To assist and automate the cross section delineation, a GIS Arc Macro Language (AML) program was developed. A total of 1,060 cross sections was calculated and incorporated into the channel configuration input file. The cross sections were normal to the channel thalweg. For each cross section, 50 horizontal width distances from bank to bank (one for each meter in elevation above the lowest channel bed elevation) were computed by the AML.

Preliminary simulations using the one-dimensional Denlinger model were made using the 1,060 channel cross sections described above. Because width changes from cross section to cross section in the Bartang and Panj Rivers are highly variable and abrupt, a one-dimensional flow model can overestimate the velocity and amplitude of the flow front (Frazao and Zech, 2002). The Riemann weighted average flux solution technique used in the Denlinger model was not formulated to incorporate large changes in cross section.

Using a two-dimensional model with the same level of cross sectional detail could have resolved these issues and provided a better estimate of delays. However, the setup costs and time necessary to use a two-dimensional model were outside the original scope of the study. Using the one-dimensional model for the study required averaging the channel width over the length of the reach. For the final simulations, the 1,060 cross sections were assumed to be rectangular with a 50-meter constant width. A 50-meter width is representative of the bottom widths of the 1,060 cross sections, which range from 5 to 1,012 meters. The mean and median of the bottom widths are 79 and 56 meters, respectively. Figure 5 shows the relationship between water depth versus both natural and constant width cross sectional areas. The natural cross sections were from 11 locations spaced every 50

kilometers between 25 and 525 kilometers downstream of Usoi dam, respectively. The straight line in the figure represents the 50-meter constant width cross section. Using a 50-meter constant width cross section to represent the study reach is a simplification of real-world conditions. However, almost all of the natural cross section lines are above the constant 50-meter cross section line. The additional error introduced using a 50-meter constant width cross section would be error on the conservative side (or the side of caution).
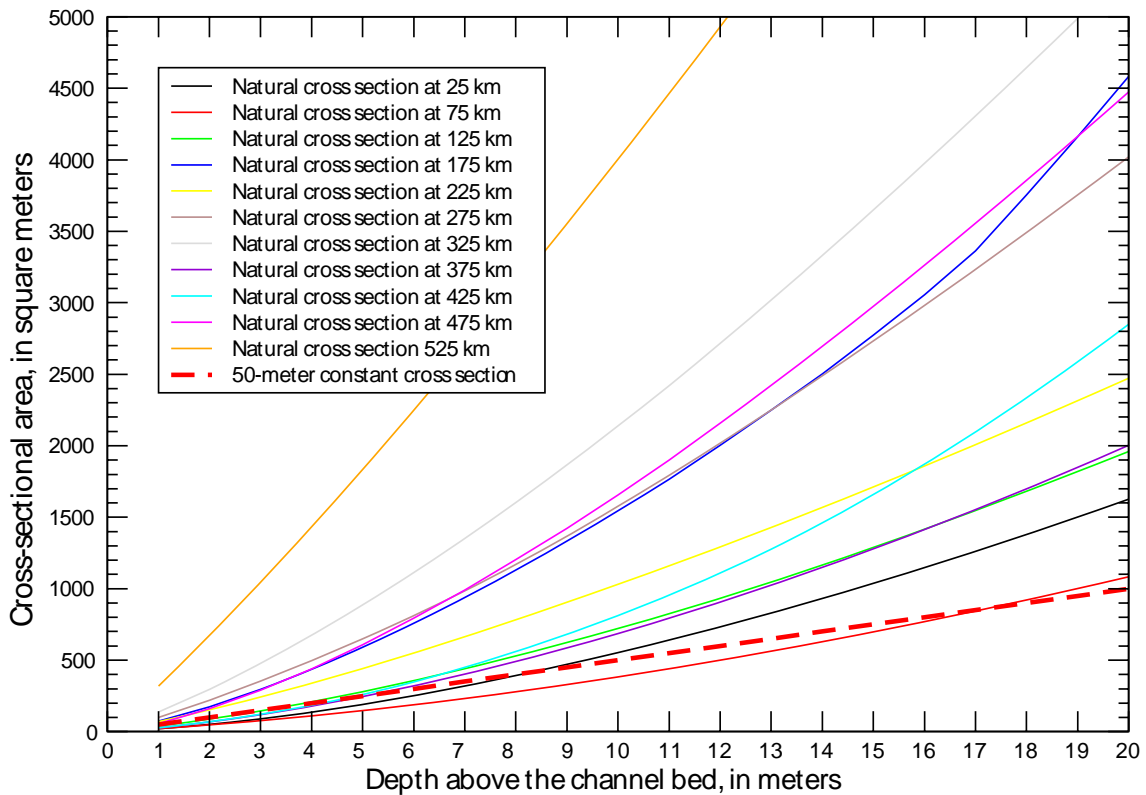
Figure 5.--Relationship between water depth and cross-sectional area.
[km, kilometers downstream of Usoi dam.]

Although the natural cross-section widths were not used in the simulations, actual thalweg elevations were included in the configuration for every 0.5 kilometer point along the reach. The numerous gradient variations within the 530 kilometer reach had a significant effect on the height and velocity of the flood wave.

Roughness Coefficients

The only available guide to determining roughness values were digital photographs of 30 reaches, located throughout the study area, taken by representatives of the FOCUS Humanitarian Assistance organization. Various stream slopes within the reach were approximated using the DEM. On the basis of the mean slope for the entire reach (approximately 0.47 percent) and the photos, a coefficient of 0.038 seemed appropriate on the basis of comparison with Barnes (1967). Therefore, a

constant roughness coefficient of 0.038 was used for all 1,060 cross sections throughout the model configuration.

Simulations

Separate flood-routing simulations were made for three overtopping flood scenarios. In addition to the overtopping floods, we simulated the worst-case scenario of a total dam breach.

Overtopping Floods

The Denlinger model simulates an upstream boundary flow input as an instantaneous collapse of water, which would be analogous to removing a giant sluice gate. Because of the way the model operates, the overtopping flood hydrographs (fig. 4) could not be used as a time-varying upstream boundary flow input. However, the hydrograph durations ranged from only 70 to 110 seconds, which could be considered near instantaneous conditions in any case. The calculated overtopping flood volumes were used to define the dimensions of the water prisms released at the dam. Height, length, and width dimensions used for each overtopping flood simulation are shown in table 3.

Table 3: Input water prism dimensions used for the overtopping flood simulations

Model specified height, in meters	Model specified length, in meters	Assumed width, in meters	Overtopping flood volume, in million cubic meters
310	129	50	2
730	600	50	22
5,000	350	50	87

The actual height and length dimensions used for the water prism were not critical so long as they and the assumed width (50 meters) corresponded with a specified overtopping flood volume used in the simulation. Using different combinations of height and length to define a flood volume only had the effect of altering the simulated flow depth profile for about 10-20 kilometers below the dam. As the simulated flood wave moves further downstream, the flow depth profiles are identical for any given combination of height and length of the water prism.

Although the length of the model time steps are variable (typically from 0.01 to 20 seconds) and determined by the numerical solution, output files from the Denlinger model are written at constant time increments (such as 7.5, 15, 30, or 60 minutes) which are preset by the user. Each output file is a "snapshot" of simulated velocity and flow depth at each half-kilometer spaced cross section for the entire 530 kilometer reach. Figure 6 shows 5-hour interval flow depth profiles for the worst case overtopping flood scenario (which has a total volume of 87,000,000 cubic meters of water) based on a constant 50-meter channel width. The simulated peak flow depths were approximately 8, 7, and 6.5 meters above the channel bed at locations 50, 100, and 150 kilometers downstream of the dam, respectively. The leading edge of the flood profile remains abrupt and nearly vertical as it moves down the reach. The combination of a near flat reach (140 to 175 kilometers downstream of the dam) and a very steep reach (175 to 195 kilometers downstream of the dam) (shown in fig. 3) had a significant

effect on the flow depth profiles because some of them have double peaks. Overall flow depth is also sharply decreased for locations downstream of 195 kilometers downstream of the dam compared to the reach between the dam and 140 kilometers downstream of the dam.
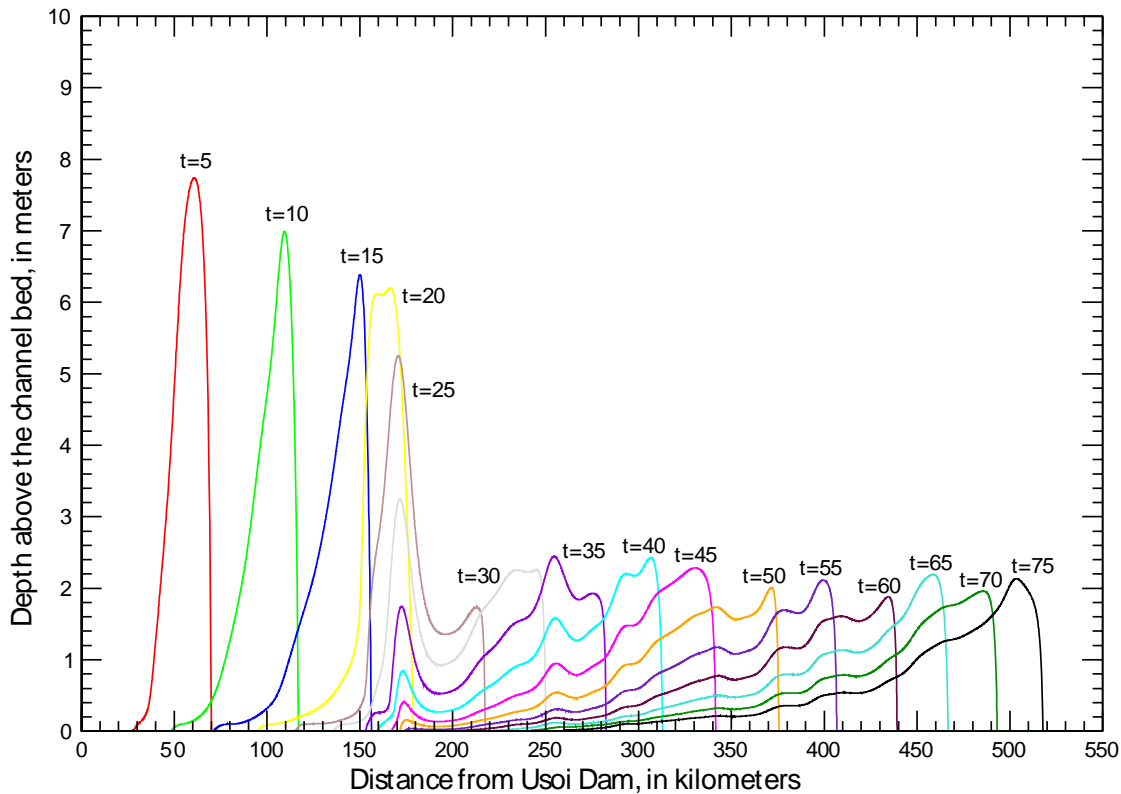
Figure 6.--Flow depth profiles of the 87 million cubic meter volume overtopping flood at 5-hour intervals.
[Notation "t=5-75" corresponds to the number of hours after the start of the flood event for each profile.]

The simulated flow depths, based on a constant 50-meter channel width, provide a coarse approximation of potential flood levels. However, for hazard mitigation it is necessary to estimate more accurate flood levels at selected locations of interest along the river. Using the constant 50-meter channel width, simulated velocity, and simulated depth, simulated flow at each cross section can be computed. The peak flow for a given location can then be used in step-backwater analysis or as input to a 2-dimensional model to determine local peak flood elevations.

Step-backwater analysis would be used for locations having subcritical flow conditions, which could be expected to occur upstream of channel constrictions or "choke" points in the study reach. (Many of the villages seem to be located in the flatter, wider subcritical flow reaches upstream of channel constrictions rather than along the narrower steep canyon-like reaches.) Because cross sections located every half-kilometer have already been created for this project, they could be used in step-backwater analyses. As an example, if the wide, flat reach located 140 to 175 kilometers downstream of the dam were used in a step-backwater analysis, the starting downstream cross section would be just upstream of the steep and narrow reach (175 to 195 kilometers downstream of the dam). The flood elevation computation would start at the downstream cross section and then work upstream one cross

section at a time. Simulated peak flow from the Denlinger model at the downstream cross section would be the flow input. For convenience, the one-dimensional HEC-RAS model is commonly used in many step-backwater analyses (U.S. Army Corps of Engineers, 1998). However, step-backwater analysis could not be used in steep gradient reaches where supercritical flow conditions are likely to occur.

A more accurate method of determining local peak flood elevations than step-backwater analysis would be to use a two-dimensional model (horizontal X and Y dimensions). A two-dimensional model could also simulate the effect of sharp channel bends on flood elevations and supercritical flow conditions. The Tidal, Residual, Intertidal Mudflat (TRIM) model has a two-dimensional version that has been used in various flood applications around the world (Casulli, 1990; Cheng and others, 1993). Setting up the model configuration necessary to use TRIM for a reach of interest could be done using the 17-meter DEM created in the study. Simulated peak flow from the Denlinger model would be the upstream boundary input to a TRIM simulation.

Simulation results from the Denlinger model for all three overtopping flood scenarios are shown in figures 7 through 9. In these figures, the peak flow was determined by extracting the maximum simulated flow that occurred at each cross section along the study reach. These figures also show the corresponding depth and velocity that occurred at the time of peak flow. As expected, the 87 million and the 2 million cubic meter volume overtopping floods produced the highest and the lowest peak flows, peak depths, and peak velocities of three scenarios, respectively. For the 87 million cubic meter overtopping flood, peak flows were approximately 1,100, 800, and 550 cubic meters per second at locations 50, 100, and 150 kilometers downstream of the dam, respectively. Peak velocities for all three overtopping floods generally ranged from 1 to 3 meters per second for most of the study reach. Velocity decreased in low channel gradient reaches such as the confluence of the Bartang and Panj Rivers (between approximately 140 and 175 kilometers downstream of the dam). However, velocity increases in the reach from 175 to 195 downstream of the dam because the channel gradient (over 1 percent) is steeper than the average for the entire study reach (0.47 percent).
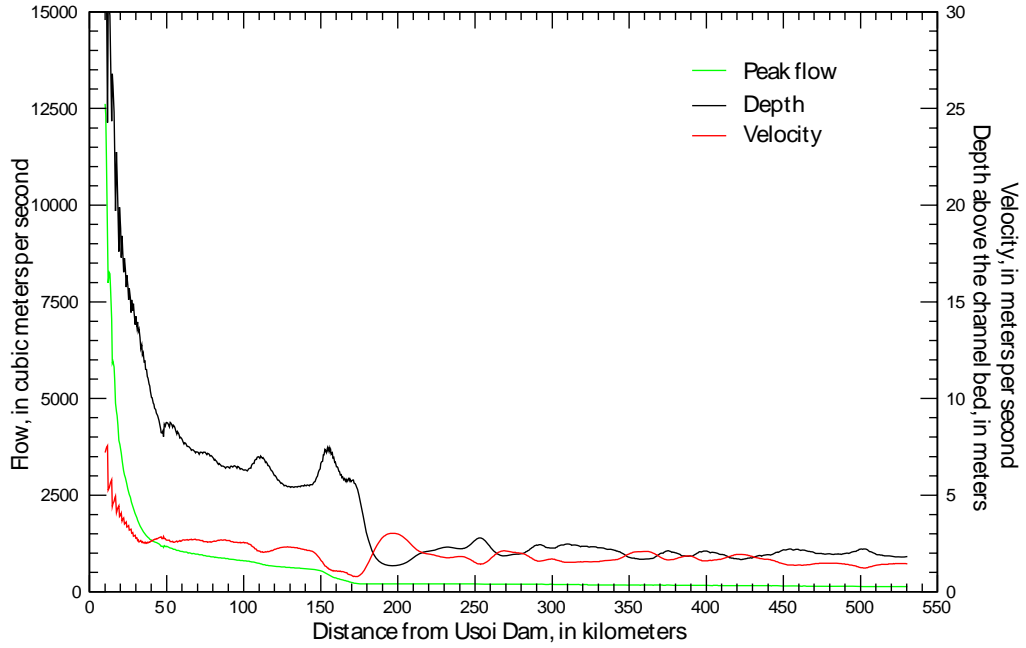
Figure 7.--Peak flow and corresponding depth and velocity for the 87 million cubic meter volume overtopping flood.
[Based on actual channel slope and hypothetical 50-meter channel width.]
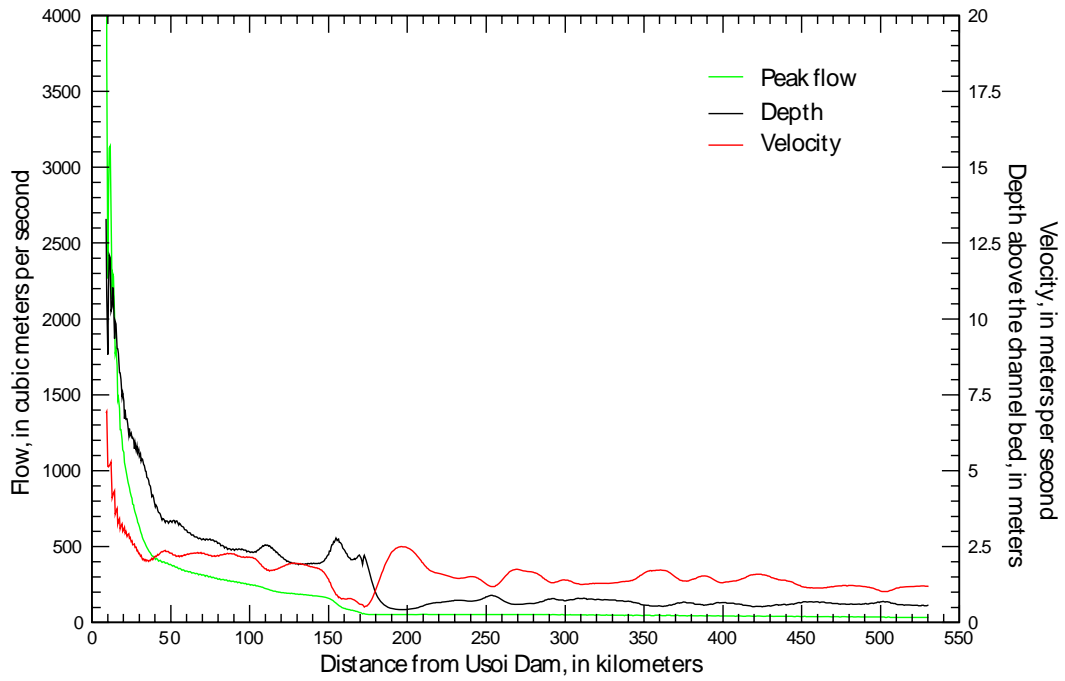
Figure 8.--Peak flow and corresponding depth and velocity for the 22 million cubic meter volume overtopping flood.
[Based on actual channel slope and hypothetical 50-meter channel width.]

15
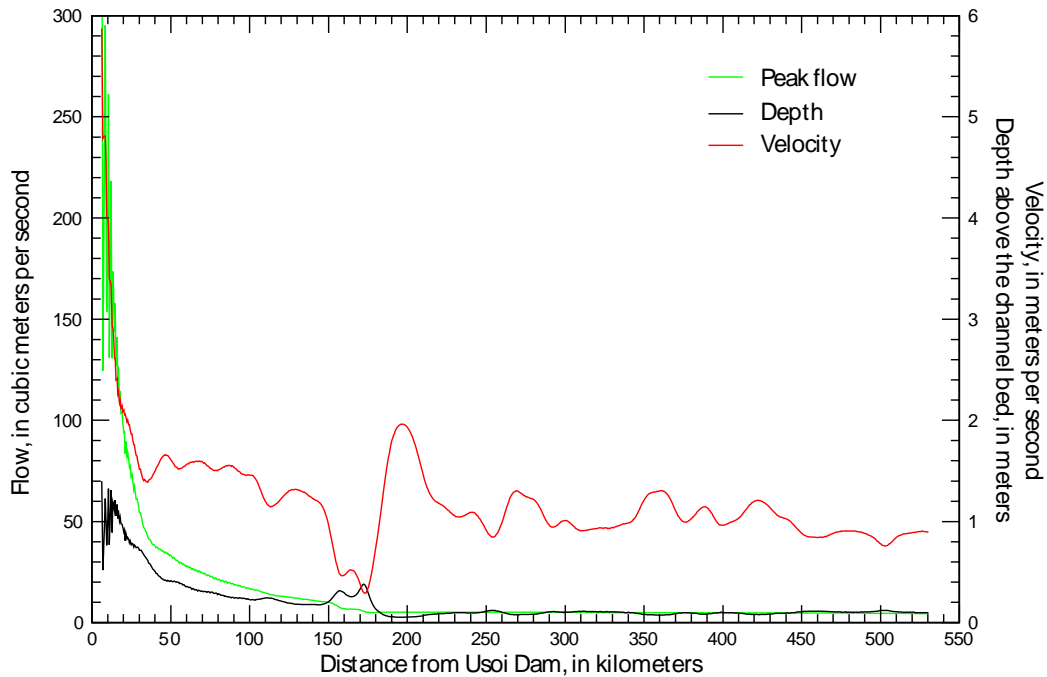
Figure 9.--Peak flow and corresponding depth and velocity for the 2 million cubic meter volume overtopping flood.
[Based on actual channel slope and hypothetical 50-meter channel width.]

The appearance of small oscillations in the lines on the left side in figures 7 through 9 is the result of the aliasing effect of the model output. The model output was provided as "snapshots" (shown in fig. 6) every 7.5 minutes. Peak flow for each cross section was extracted from an overlay of all the snapshots. Because of the speed of the flood wave, a 7.5-minute increment of output was not able to always capture the peak flow that the model really simulated at some locations. True peak flow would appear on figures as a smoother line connecting the peaks of the oscillations. Peak flow, depth, and velocity between the dam and 10 kilometers downstream of the dam are not shown in figures 7 through 9 because the extreme velocity of the flood wave in this reach created extreme oscillations in the model output. The nearest village, Barchidev, is 16 kilometers downstream of the dam.

In addition to knowing an approximate location and extent of the flood elevation, hazard mitigation planners need to know the approximate arrival time of the flood wave at points along the reach. Figure 10 shows the wetting front arrival times for the three overtopping floods. The wetting front arrival times for the 2, 22, and 87 million cubic meter volume overtopping floods at the lower end of the reach are approximately 135 (5.6 days), 95 (4 days), and 77 (3.2 days) hours, respectively.

16
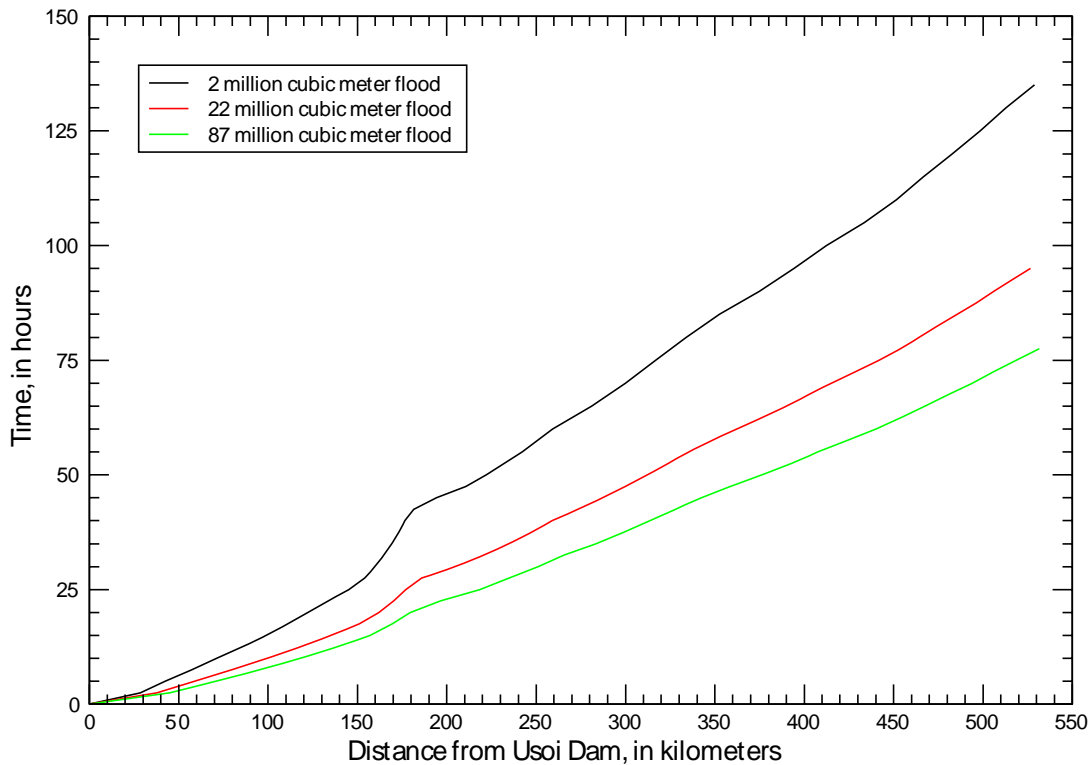
Figure 10.--Wetting front arrival times of the three overtopping floods.

Dam-Breach Flood

Although complete and rapid breaching of the dam is unlikely according to the geotechnical analyses of Hanisch and Soder (2000) and Stucky Consulting Engineers (2001), the resulting flood would be the worst-case scenario. The geotechnical studies by Hanisch and Soder (2000) and Stucky Consulting Engineers (2001) suggest that the Usoi dam is unlikely to fail owing to either seismic shaking or ground-water seepage forces. However, an overtopping flood wave of sufficient size could erode the blockage enough to initiate a breach. As described earlier, for breach erosion rates ranging between 10 and 100 meter per hour, the entire lake would empty in 4.1 to 36.3 hours, resulting in a peak discharge between 0.26 and 2.3 million cubic meters per second. However, because input hydrographs can not be specified for the Denlinger model, it was not possible to specifically evaluate these two end-member dam-breach hydrographs. The U.S. National Weather Service FLDWAV model may be capable of simulating the two dam-breach hydrographs; although we did not attempt to do this due to time and budget limitations.

For this study, we used the Denlinger model to simulate the flood wave that would result from an instantaneous breaching of Usoi Dam and complete draining of Lake Sarez. This is not as physically plausible as the previously described dam-breach scenarios, but it does provide information on the maximum possible hazard. Because the total volume of the dam breach flood (17 cubic kilometers) is many times greater than the volumes of the overtopping floods, it was necessary to

17

assume a much larger water prism for the upper boundary in the simulation. For the height of the prism (at the upstream boundary) we used 500 meters because that is the approximate height of Usoi dam. Length of the prism was specified at 34,000 meters. However, instead of using a constant 50-meter width rectangular channel as we used in the overtopping flood simulations, it was necessary to assume a wider constant (1,000-meter) width rectangular channel. To use a 50-meter-wide rectangular channel would have required using an unrealistic prism length dimension (680,000 meters). Also, it would have been unrealistic to assume that the width of a flood from an instantaneous dam breach would not be wider than 50 meters. Because of the length of the prism (34,000 meters), the reach from 0 to 34 kilometers downstream of the dam could not be simulated. The upper boundary started at 34 kilometers downstream of the dam.

Results from the dam-breach flood scenario simulation are shown in figure 11. Simulated peak flows were approximately 64,000, 52,000, 40,000, and 20,000 cubic meters per second at locations 50, 100, 150, and 530 kilometers downstream of the Usoi dam. Figure 11 also shows the corresponding depth and velocity for the dam-breach flood scenario. The wetting front arrival time at the lower end of the study reach was approximately 56 hours (2.3 days) (fig. 12), which is sooner than the wetting front arrival times of the overtopping floods.
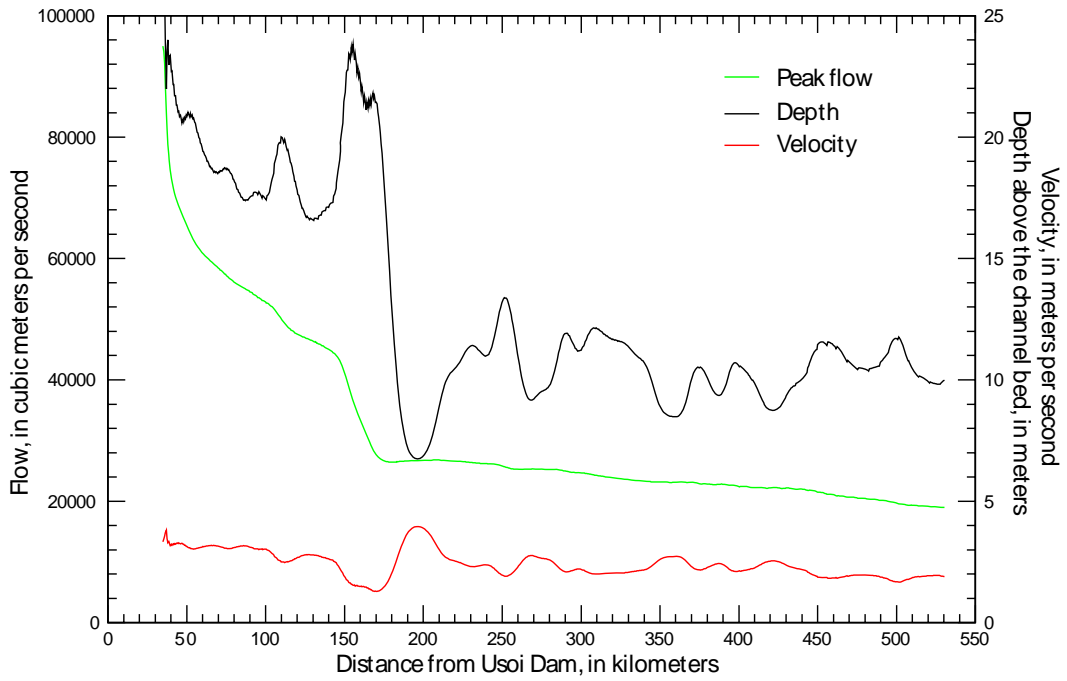
Figure 11.--Peak flow and corresponding depth and velocity for the dam-breach flood.
[Based on actual channel slope and hypothetical 1000-meter channel width.]
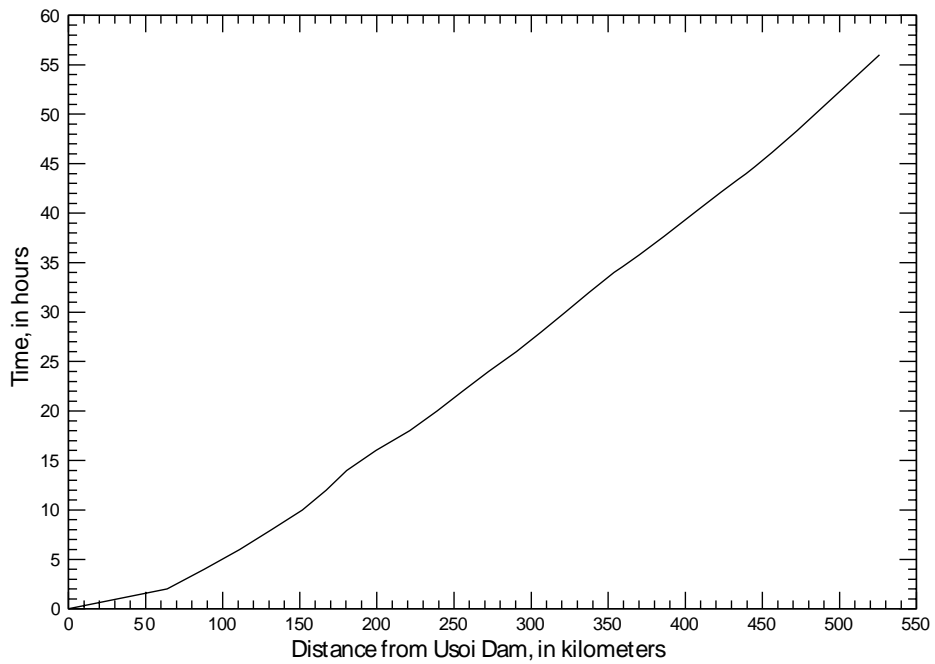
Figure 12.--Wetting front arrival time of the dam-breach flood.

As expected, the magnitude of the peak flow from the dam-breach flow is significantly greater than the peak flow from the largest overtopping flood (87 million cubic meters) scenario. The peak flow information shown in figure 11 can be used in conjunction with step-backwater analysis or two-dimensional modeling (both described earlier) to determine local peak flood elevations for a location of interest. Because the results shown in figure 11 were simulated using a constant 1,000-meter wide channel, which is wider than the average bottom width for the actual study reach channel, it can be assumed that these peak flows would be higher than the peak flows from a simulation based on the actual channel bends and contractions in the study reach. However, estimated peak flood elevations based on higher peak flows would be error on the side of caution.

Limitations

Owing to the many approximations involved in developing the starting hydrographs, due caution should be used in interpreting results of the flood-routing simulation. For the overtopping flood scenario, we have described the wave-generation process by a method consistent with scale-model experiments, but we have made no attempt to calculate the evolution of the wave geometry as it propagated toward the dam; doing so would require detailed lake bathymetric data, which was unavailable.

Similarly, we have relied upon actual scale-model experiments and, to some extent, theory in calculating wave runup on the dam and the volume of water that would overtop and enter the channel downstream. Such scale-model experiments do not incorporate all the complex topography in real landslide dams. For the dam breaching scenario, we assumed total drainage of the lake. Although this commonly occurs when earthen dams fail, many natural dams only breach partially, therefore releasing only a portion of the impounded volume. Additionally, landslide dams are commonly broader than other earthen dams, such as constructed or moraine dams, and erosion rates applicable for breaching of landslide dams may be lower than the rates used in arriving at the hydrograph characteristics in table 2 (Walder and O'Connor, 1997).

Assuming that an exact input flood hydrograph could be predicted, there are still other limitations with the simulations. Although 0.5-kilometer-spaced cross sections were calculated and used in preliminary simulations, they were not be used in the final simulations because of numerical difficulties in propagating the flood wave downstream. It was necessary to assume constant 50-meter rectangular cross sections for the entire reach in the overtopping flood simulations; however, actual elevation detail was included in the simulations.

The model used in this study was one-dimensional. The 530 kilometer Bartang and Panj River study reach contains numerous bends. The possible effects of sharp bends cannot be accounted for in a one-dimensional model. In a sharp bend, the centrifugal forces in a high velocity flow will cause the depth to be higher on the outside than on the inside of the turn. A two-dimensional flood-routing model would be more accurate in simulating the maximum flood levels.

The flood-routing simulations also assumed a constant roughness coefficient for the entire length of the study reach. A value of 0.038 was used because it is representative of mountainous streams similar to the Bartang and Panj Rivers. However, the flood-routing simulations might have been more accurate if separate roughness coefficients were used for different sections of the study reach. To properly estimate roughness coefficients, the Manning's equation can be used if discharge time series data are available at two or more locations.

The simulations were based on clear water conditions and did not simulate changes to the channel geometry that could occur due to scour and deposition. Outburst floods from the Usoi dam would undoubtedly entrain and deposit material along the flood route, which would probably increase the flow volume.

Summary and Conclusions

In the winter of 1911 a massive rock slide in the Pamir Mountains of southeastern Tajikistan completely blocked the valley of the Bartang River and formed the world's highest natural or man-made dam, which today impounds approximately 17 cubic kilometers of water in Lake Sarez.

Previous geotechnical studies suggest that the Usoi dam itself is unlikely to fail owing to either seismic shaking or ground-water seepage forces. Therefore, the likeliest scenario for a flood would be from landslides entering the lake that produce waves capable of overtopping the dam and entering the channel downstream. A rock mass on the right-bank slope of the lake, approximately 3 kilometers from the dam, is known to be a potential source of a wave-generating landslide.

A set of hypothetical flood hydrographs were developed based on a plausible range of volumes of landslide material that could fall into the lake. For landslide volumes of 200, 500, and 1,000 million cubic meters, estimated overtopping flood volumes were 2, 22, and 87 million cubic meters, respectively. Estimated peak discharge for these three flood scenarios were 57,000, 490, 000, and 1,580,000 cubic meters per second based on triangular hydrographs of 70, 90, and 110 second durations, respectively.

Flood-routing simulations were made for the three landslide-induced overtopping floods and a worst-case scenario of the entire dam breaching for the 530 kilometer reach of the Bartang and Panj Rivers below the Usoi dam. The flood routing was performed with a one-dimensional flow model using a Riemann numerical solution technique. The channel hydraulic characteristics included a roughness coefficient of 0.038 (appropriate for steep mountainous streams) and actual elevations for every 0.5 kilometer point along the reach. Cross sections were assumed as rectangular in shape with a constant 50-meter width.

For the maximum overtopping flood scenario, having a volume of 87 million cubic meters, the estimated peak flows were approximately 1,100, 800, and 550 cubic meters per second at locations 50, 100, and 150 kilometers downstream of the dam, respectively. Such a flood would cause elevated flow stages throughout the entire 530-kilometer study reach. As expected, the simulated peak flows for the two other overtopping flood scenarios were lower than the maximum overtopping flood scenario. To accurately determine local peak flood elevations for a location of interest, simulated peak flows from this study can be used boundary input data to a step-backwater analysis or as input to a 2-dimensional model.

Though less probable than an overtopping flood, the worst-case flood scenario would be a complete dam breach and draining of the lake (17 cubic kilometers). The resulting flood, which would have a volume many times greater than the overtopping flood volumes, would have greater discharges and velocities, and would persist for a longer duration. Simulated peak flows were approximately 64,000, 52,000, 40,000, and 20,000 cubic meters per second at locations 50, 100, 150, and 530 kilometers downstream of the Usoi dam, respectively.

References Cited

Alford D., 2000, Flood Scenarios, *in* Alford, D. and Schuster, R., eds., 2000, Usoi Landslide Dam and Lake Sarez—An Assessment of Hazard and Risk in the Pamir Mountains, Tajikistan: Geneva, Switzerland, United Nations, International Strategy for Disaster Reduction (ISDR) Prevention Series No. 1 (ISBN 92-1-132022-4), Chapter 6, p. 59-62.

Alford D. and Schuster, R., 2000, Introduction and summary, *in* Alford, D. and Schuster, R., eds., 2000, Usoi Landslide Dam and Lake Sarez—An Assessment of Hazard and Risk in the Pamir Mountains, Tajikistan: Geneva, Switzerland, United Nations, International Strategy for Disaster Reduction (ISDR) Prevention Series No. 1 (ISBN 92-1-132022-4), Chapter 1, p. 1-18.

Barnes, H.H., 1967, Roughness characteristics of natural channels: U.S. Geological Survey Water-Supply Paper 1849, 213 p.

Casulli, V., 1990, Semi-implicit finite-difference methods for the two-dimensional shallow water equations: Journal of Computer Physics, v. 86, p. 56-74.

Cheng, R. T., Casulli, V., and Gartner, J.W., 1993, Tidal, residual, intertidal mudflat (TRIM) model and its applications to San Francisco Bay, California: Estuarine, Coastal, and Shelf Science, v. 36, p. 235-280.

Clague, J.J., and Evans, S.G, 1994, Formation and failure of natural dams in the Canadian Cordillera: Geological Survey of Canada, Bulletin 464, 35 p.

Costa, J.E., 1991, Nature, mechanics, and mitigation of the Val Pola Landslide, Valtellina, Italy, 1987-1988: Z. Geomorph. N.F., Marz 1991, p. 15-38.

Costa, J.E., and Schuster, R.L., 1991, Documented historical landslide dams from around the world: U.S. Geological Survey Open-File Report 91-239, 486 p.

Dean and Dalrymple, 1991, Water wave mechanics for engineers and scientists: Singapore, World Scientific, 353 p.

DeLong, L.L., Thompson, D.B. and Lee, J.K., 1997, The computer program FourPt (Version 95.01)—A model for simulating one- dimensional, unsteady, open-channel flow: U.S. Geological Survey Water-Resources Investigations Report 97-4016, 69 p.

Denlinger, R., and Iverson, R., 2001, Flow of variably fluidized granular masses across three-dimensional terrain 2. Numerical predictions and experimental tests: Water Resources Research, v. 106, no. B1, p. 553-566.

Fan, G., Ni, J. F., and Wallace, T. C., 1994, Active tectonics of the Pamirs and Karakoram: Journal of Geophysical Research, Solid Earth, v. 99, no. Be, p. 7131-7160.

Frazao, S. S., and Zech, Y., 2002, Dam break in channels with a 90 degree bend, Journal of Hydraulic Engineering, v. 128, issue 11, p. 956-968.

Fread, D.L. and Lewis, J.M., 1998, NWS FLDWAV MODEL: National Weather Service, [http://www.nws.noaa.gov/oh/hl/rvmech/documentation/fldwav_doc.pdf, accessed May 21, 2001.]

Hanisch, J. and Soder, C., 2000, Geotechnical assessment of the Usoi landslide dam and right bank of the Lake Sarez, *in* Alford, D. and Schuster, R., eds., 2000, Usoi Landslide Dam and Lake Sarez—An Assessment of Hazard and Risk in the Pamir Mountains, Tajikistan: Geneva, Switzerland, United

Nations, International Strategy for Disaster Reduction (ISDR) Prevention Series No. 1, (ISBN 92-1-132022-4), Chapter 3, p. 23-42.

Huber, A., 1980, Schwallen in Seen als Folge von Felssturzen: Zurich, VAW-ETH, Mitt. Nr. 47.

Ives, J. and Pulatova, G., 2000, Human Geography/Demography *in* Alford, D. and Schuster, R., eds., 2000, Usoi Landslide Dam and Lake Sarez—An Assessment of Hazard and Risk in the Pamir Mountains, Tajikistan: Geneva, Switzerland, United Nations, International Strategy for Disaster Reduction (ISDR) Prevention Series No. 1, (ISBN 92-1-132022-4), Chapter 9, p. 83-86.

Jobson, H.E., 1989, Users manual for an open-channel streamflow model based on the diffusion analogy: U.S. Geological Survey Water-Resources Investigations Report 98-4133, 73 p.

Muller, D.R., 1995, Auflaufen and Uberschwappen von Impulswellen an Talsperren: Zurich, VAW-ETH, Mitt. Nr. 137.

O'Connor, J.E., Hardison, J.H., and Costa, J.E., 2001, Debris flows from failures of neoglacial-age moraine dams in the three sisters and Mount Jefferson Wilderness areas, Oregon: U.S. Geological Survey Professional Paper 1606, 93 p.

Stucky Consulting Engineers, 2001, Lake Sarez Risk Mitigation Project—Design Report (ID67610), A—Monitoring and early warning systems and C—Studies on long-term solutions: Renens, Switzerland, PD/cb/4448/4006a, [variously paginated].

Synolakis, C.E., 1987, The runup of solitary waves: Journal of Fluid Mechanics, 185, p. 523-545.

Synolakis, C.E., 1991, Tsunami runup on steep slopes—How good linear theory really is: Natural Hazards, vol. 4, p. 221-234.

Toro, E.F., 1997, Riemann solvers and numerical methods for fluid dynamics: Springer-Verlag Publishers, 592 p.

U.S. Army Corps of Engineers, 1998, HEC-RAS river analysis system, version 2.2: Hydraulic Reference Manual CPD-69, [variously paginated].

Vreugdenhil, C.B., 1994, Numerical methods for shallow water flow: Klumer Academic Publishers, 261 p.

Walder, J.S., Sorenson, O.E., and Watts, P., in press, Water waves generated by subaerial mass flows, Journal of Geophysical Research.

Walder, J.S., and O'Connor, J.E., 1997, Methods for predicting peak discharge of floods caused by failure of natural and constructed eathen dams: Water Resources Research., v. 33, p. 2337-2348.

Watts, P., 2001, Tsunami Open and Progressive Initial Conditions System (TOPICS), program, freeware available through Applied Fluids Engineering, Inc., Private Mail Box #237, 5710 E. 7th Street, Long Beach, California, 90803, http://www.appliedfluids.com/

Watanabe, T., 2000, Environmental impact assessment—Geomorphology of the Bartang and Kudara valleys *in* Alford, D. and Schuster, R., eds., 2000, Usoi Landslide Dam and Lake Sarez—An Assessment of Hazard and Risk in the Pamir Mountains, Tajikistan: Geneva, Switzerland, United Nations, International Strategy for Disaster Reduction (ISDR) Prevention Series No. 1, (ISBN 92-1-132022-4), Chapter 5, p. 53-58.

Appendix A: Alternative Investigation

An alternative method of estimating landslide induced overtopping flood is presented in Stucky Consulting Engineers (2001). Stucky Consulting Engineers (2001) concluded that an overtopping flood was unlikely to occur for landslides with a volume less than 500 million cubic meters. The authors evaluated two scenarios of overtopping floods that could be caused by potential landslides having 100 and 500 million cubic meters of material. The calculated overtopping flood volumes were 9,000 and 1,567,000 cubic meters for landslides that are 100 and 500 million cubic meters in size, respectively. For the 9,000 cubic meter flood, its volume would be completely absorbed by the blocks of material on the dam crest before the flood reached the downstream face of the dam. For the 1,567,000 cubic meter flood, more than 50 percent of its volume would be absorbed by two depressions on the dam crest, which would have created small lakes on the southern side of the crest.

For the two scenarios of 200 and 500 million cubic meters of landslide material, the calculated volume of overtopping floods in our study was 2,000,000 and 22,000,000 cubic meters, respectively. It is possible and likely that some of the overtopping flood volume could be absorbed by the two dam crest depressions. Not having access to detailed topographic data on Usoi Dam, we did not assume or estimate flood volume losses to the dam crest depression in our simulations.

The main reason our study and the study by Stucky Consulting Engineers (2001) had differing overtopping flood volumes was due to very different estimates of the flood wave amplitude that would occur in the vicinity of the landslide. Our study estimated wave amplitude heights that were typically twice as high as comparable wave heights estimated by Stucky Consulting Engineers (2001). Both studies used different methods of calculating wave amplitude. The approach in our study used empirically derived equations based on laboratory data. Wave amplitude was defined as a function of landslide volume (V), water depth of the lake (h), lake width (W), and duration of landslide motion (t_o) (Appendix B).

Stucky Consulting Engineers (2001) assumed that the ratio of landslide and wave energies could be constant for different events. Using observed data from historic events that took place at Flores Island, Indonesia, and Morrow Point Dam, Colorado, they assumed that the ratio landslide and wave energies could then be applied to Lake Sarez. However, wave energy was computed using a sinusoidal wave equation that did not use lake depth as an input. Water depths where the historic landslide events took place were shallower than the Lake Sarez site (300 meters).

Appendix B: Method of Estimating the Starting Hydrograph for the Overtopping Flood Scenarios

We use a three-step procedure to estimate the starting hydrograph, that is, the hydrograph at the Usoi dam. This procedure entails distinguishing three phenomena: wave generation, wave runup against an adverse slope, and wave overtopping. Wave generation is assessed using the experimentally based scaling results of Walder and others (in press) to predict the "near-field" wave amplitude associated with a particular size landslide. Wave amplitudes predicted by this method strictly apply only to a two-dimensional (flume-like, using x and z dimensions) geometry, so an approximate correction for geometrical spreading must be applied. For this purpose, we apply the method described in the TOPICS software package (Watts, 2001). Wave runup on the Usoi dam is then estimated using Synolakis' (1987) theoretical results for runup of solitary waves. This theory has been shown to describe experimental data reasonably well (Synolakis, 1991). Although the landslide-generated

impulse waves are probably not strictly solitary waves, the leading wave will probably have a shape similar to that of a solitary wave, so applying Synolakis' results should be reasonably accurate. Finally, wave overtopping is assessed using Müller's (1995) scaling results based on laboratory tests. These three steps are described in further detail below.

Wave generation and propagation

We assume that waves are generated by a landslide from one of the banks, and that waves propagate towards both the Usoi dam and the upvalley end of the lake. Walder and others (in press) have shown that a coherent wave first exists in the "near field," which is the region just beyond the "splash zone" of complicated fluid/solid interaction, but before propagation effects—dispersion, bathymetric refraction, and wave-front spreading—come into play. Although the near-field region is spatially limited, it turns out that for many impulse waves in lakes, much of the domain of interest lies within the near field. Moreover, the near-field impulse wave has well-defined characteristics and can serve as a proxy "source" for computational wave-propagation purposes. Thus as long as one is willing to forego details of the conditions within the splash zone proper—and that is appropriate for the present application—then the wave-propagation part of the impulse-wave problem can be carried out independently of the complicated exercise of computing splash-zone dynamics.

We begin by summarizing results for wave generation in constant-depth, flume-like channels. The near-field wave has some local amplitude $\eta(x)$, where x is distance in the direction of landslide motion. Walder and others (in press) have shown that experimental data for maximum wave height η_{max} in the near field are well described by

$$\frac{\eta_{max}}{h} = 1.32 \left(\frac{V_w{}^*}{t_s{}^*} \right)^{0.68}$$
(1)

where h is water depth. Vw^* is a dimensionless measure of wavemaker volume per unit lake width:

$$Vw^* = V/Wh^2$$
(2)

where V is wavemaker volume and W is landslide width. The term "wavemaker" is commonly used in the coastal-engineering literature (e.g., Dean and Dalrymple,1991) and we adopt it here. The dimensionless duration of landslide motion, ts^*, is defined by

$$t_s{}^* = t_s \left(\frac{g}{h} \right)^{1/2}$$
(3)

where ts is duration of landslide motion and g is acceleration of gravity. Equation (1), which applies up to the stability limit $\eta_{max}/h \approx 0.85$, appears to be generally valid for diverse types of laboratory wavemakers, including solid blocks and dry granular avalanches, and we shall assume that it applies to rock avalanches in nature.

The near-field wave is commonly a broad hump with "wavelength" λ –really a measure of the hump's width–given empirically by

$$\frac{\lambda}{h} = 0.27 t_s{}^*$$
(4)

when the wave shape is fit to a function $\eta(x) = \eta_{max} sech^2(x/\lambda)$.

Equations (1) to (4) strictly apply to constant-depth, flume-like (that is, two-dimensional, constant-depth) channels. For prognostic purposes such as the present one, Vw^* can be calculated once one specifies V, W and h. Geotechnical considerations can be used to posit plausible values of V and W; h should be interpreted as the depth at which the landslide stops. Estimating ts or ts^* requires some additional considerations. Walder and others (in press) found in their block-landslide experiments that

$$t_s^* = 4.5 \left(\frac{L}{h}\right)^{0.5} \tag{5}$$

where L was the length of the block landslide. For actual landslides, L is of course not known in advance, but we can make plausible estimates by assuming that a landslide of total volume V will spread out with a characteristic lateral extent L and thickness εL , where $\varepsilon \ll 1$. We then find $V = \varepsilon L^3$ and thus

$$L = \left(\frac{V}{\varepsilon}\right)^{1/3} \tag{6}$$

so that

$$t_s^* = \frac{4.5}{\varepsilon^{1/6}} \left(\frac{V}{h^3}\right)^{1/6} \tag{7}$$

In what follows we will use Equation (7) with the value $\varepsilon = 0.1$, corresponding to a rather blunt landslide. Smaller values of ε may be more reasonable in many situations, so we are probably underestimating ts^* and λ/h and overestimating wave amplitude. Note, however, that $ts^* \sim \varepsilon^{1/6}$, so a tenfold change in *epsilon* changes ts^* by a factor of only about 1.5.

Equations (1) to (7) would suffice for a natural geometry akin to a flume–that is, a long, narrow water body with the landslide source at one end. The situation at Lake Sarez differs from a flume in an obvious way: the likely landslide sources are along the banks. In the lake, the landslide creates a near-field lateral wave mound (or "hump") of water that spreads both upvalley and downvalley. Therefore, to determine the appropriate wave height, it was necessary to double the volume of material that fell into the lake and use the wave height, calculated from the flume analyses, that was associated with that volume. To deal with lateral wave spreading, we assumed that the near-field wave source evolved into more or less circular mound. For an assumed wave shape $\eta(r) = sech^2(r/\lambda)$ with r being radial distance from the peak, volume conservation requires that

$$\frac{\eta_{max}}{h} = \frac{V}{4h\lambda^2} \tag{8}$$

and using Equations (4) and (7),

$$\frac{\eta_{max}}{h} \approx 0.078 \left(\frac{V}{h^3}\right)^{2/3} \tag{9}$$

The amplitude of the leading wave will decrease with distance from the generation zone owing to dispersion and other effects. The near-field amplitude described above should be reasonably accurate out to a distance of about $3\hat{L}$ from the generation zone (cf. Watts, 2000), where $\hat{L} = t_s * h$ is the "width" of the waveform. At greater distances, wavefront spreading reduces wave amplitude noticeably (Huber, 1980). $\hat{L} = 0.5 - 1.5 km$ for plausible ranges of V and ε and h = 350 m, a typical lake depth in the region of interest. With the likeliest landslide source being about 3 to 4 km from the dam, the wave amplitude estimated by the method probably modestly overestimates wave amplitude at the dam. A more detailed calculation would involve solving the nonlinear partial differential equations for wave propagation, with detailed bathymetry being one of the inputs required for the calculation.

Wave runup

We will assume as a reasonable approximation that Synolakis' (1987, 1991) results for runup of solitary waves are applicable to the impulse waves of interest here. Synolakis predicted on theoretical grounds—and laboratory data show this result to be reasonably accurate—that the runup height R of a solitary wave on a embankment with slope angle θ is given by

$$\frac{R}{h} = 2.83(cot\theta)^{1/2}\left(\frac{\eta_{max}}{h}\right)^{5/4}$$

(10)

R here should be interpreted as the runup that would occur on a sloping plane of indefinite extent. Equation (10) seems to be reasonably accurate for R/h up to approximately unity. In any actual case of interest, if R exceeds f, the freeboard (or elevation difference between the embankment crest and undisturbed water level), the wave will overtop the embankment.

For the Usoi dam, we adopt the value $\theta = 23^\circ$ as an approximate value to characterize the lakeward-facing slope. Combining Equations (9) and (10) then gives

$$\frac{R}{h} \approx 0.18\left(\frac{V}{h^3}\right)^{5/6}$$

(11)

We emphasize that this equation is valid only for $R/h < circa$ 1; in the present case, this means the limit of validity in terms of landslide volume is $V/h^3 \approx 7.8$.

Overtopping

We apply the results of Müller (1995) to get at the overtopping characteristics. Müller did flume experiments with solitary waves generated by a falling mass and dam experiments with diverse embankment slopes and crest widths. He found little dependence of overtopping volume on embankment slope and crest width. The overtopping volume Vf per unit embankment width was given by

$$\frac{V_f}{V_o} = \left(1 - \frac{f}{R}\right)^{11/5}$$

(12)

where f is the freeboard, R is (as before) wave runup, and $V0$ is a reference value, namely, the overtopping volume per unit width for $f = 0$, no freeboard. Equation (12) is obviously not meaningful if $f = h$, meaning there is no water impounded behind the dam. $V0$ is given by

$$V_o = c_o(2g\eta^3)^{1/2}\tau_o V_E \qquad (13)$$

where *co* is an O(1) empirical "weir" coefficient, τ_o is the duration of overtopping, and *VE* is another empirical coefficient of O(1). In dimensionless form this may be written as

$$\frac{V_o}{h^2} = 2^{1/2}c_o V_E\left(\frac{\eta}{h}\right)^{3/2}\tau_o\left(\frac{g}{h}\right)^{1/2} \qquad (14)$$

The coefficient *VE* is given empirically by

$$V_E = \left(\frac{4}{15}\right)\left(\frac{h}{H}\right)^{1/6} \qquad (15)$$

where *H* is the peak-to-trough wave amplitude, not generally the same as η, although for the solitary waves of interest here, the difference is small: $\eta = 0.96H$, and thus

$$V_E = 0.265\left(\frac{h}{\eta}\right)^{1/6} \qquad (16)$$

In addition, overtopping duration at zero freeboard is related to wave period *T* by the empirical relation

$$\tau_0\left(\frac{g}{h}\right)^{1/2} = 4\left[T\left(\frac{g}{h}\right)^{1/2}\right]^{4/9} \qquad (17)$$

The wave period *T* is related to the "width" $\hat{L}$ of the waveform by

$$T \approx \frac{\hat{L}}{[g(\alpha h + \beta\eta)]^{1/2}} \qquad (18)$$

where $\alpha = 0.89$, $\beta = 1.13$. The denominator is the wave celerity, which would be simply $\sqrt{gh}$ for small-amplitude "long" waves, but has a more complicated functional dependence for finite-amplitude waves. Combining Equations (14) through (18) with Equation (7) and the definition (Walder and others, in press) $\hat{L} = t_s{}^* h$, we find after some algebra:

$$\frac{V_o}{h^2} \approx 1.5\frac{(\eta/h)^{4/3}}{[\alpha + \beta(\eta/h)]^{2/9}}\left(\frac{V}{h^3}\right)^{2/27} \qquad (19)$$

The numerical coefficient in Equation (19) reflects the choice *co = 0.43*, corresponding to the case of a fairly broad-crested dam (cf. Müller, 1995). Finally, then, combining Equations (9), (12), and (19), we find the overtopping volume per unit width as a function of landslide volume *V*, water depth *h,* and freeboard *f*:

$$\frac{V_f}{h^2} \approx \frac{0.05(V/h^3)^{26/27}}{[1 + 0.1(V/h^3)^{2/3}]^{2/9}}\left(1 - \frac{5.6(f/h)}{(V/h^3)^{5/6}}\right)^{11/5} \qquad (20)$$

Note that there is a minimum landslide volume *Vmin* for any overtopping at all:

$$\frac{V_{min}}{h^3} = \left[5.6 \left(\frac{f}{h} \right) \right]^{6/5} \tag{21}$$

For the Usoi dam, supposing that $f \approx 50$ and $h \approx 350$ m are representative values, and recalling that the "effective" landslide volume needs to be doubled to account for wave propagation both up-valley and down-valley, we find no overtopping at all unless *Vmin* > circa 66 x 10^6 m^3.

The duration of overtopping at zero freeboard may be written, after some algebra, as

$$\tau_o \left(\frac{g}{h} \right)^{1/2} = 9.5 \left(\frac{(V/h^3)^{1/6}}{[1 + 0.1(V/h^3)^{2/3}]^{1/2}} \right)^{4/9} \tag{22}$$

Müller (1995) provides no data bearing on how the duration of overtopping is reduced for non-zero freeboard. Equation (21) will obviously overestimate the duration of overtopping at nonzero freeboard, but this is of negligible importance for flood-inundation calculations except very near the dam. Moreover, in the context of the other approximations involved in our approach, there seems to be no point in trying to "refine" Equation (22).

Appendix C: Method of Estimating the Starting Hydrograph for the Dam-Breach Flood Scenario

Walder and O'Connor (1997) presented a simple, physically based model of floods due to earthen-dam failures (both natural and constructed) and showed that model predictions of peak discharge were in reasonably good agreement with data, without resorting to any fitting coefficients. They showed that both peak discharge *Qp* and the time to peak, *tp*, depend primarily on lake volume *V*, the drop in water level *d*, and *k*, the mean rate of breach downcutting. *Qp* and *tp* take different asymptotic forms depending upon whether the dimensionless quantity $\eta = kV/g^{1/2}d^{7/2}$ (where *g* is acceleration due to gravity) is large or small compared to unity. In the case of Lake Sarez, using *V* = 17×10^9 m^3, *d = 350 m*, g = 9.8 m/s^2, and *k* in the range 10 to 100 m/h–corresponding to most actual dam failures–we find $\eta = 0.019$, to 0.19. We then apply the appropriate relationships from Walder and O'Connor for the case $\eta \ll 1$:

$$Q_p = 1.51(gd^5)^{0.03} \left(\frac{kV}{d} \right)^{0.94} \tag{23}$$

$$t_p = 1.24 \left(\frac{V}{k^2(gd)^{1/2}} \right)^{1/3} \tag{24}$$

Numerical values given in the main text are derived from this relation.